

Synthesis of Germanium Dioxide Microclusters on Silicon Substrate in Non-Aqueous Solution by Electrochemical Deposition

Mastura Shafinaz Zainal Abidin^{*1}, Shahjahan², Abdul Manaf Hashim³

¹Faculty of Electrical Engineering, Universiti Teknologi Malaysia, 81310 Skudai, Johor Malaysia

^{2,3}Malaysia-Japan International Institute of Technology, Universiti Teknologi Malaysia, 54100 Kuala Lumpur, Malaysia

*Corresponding author, e-mail: m-shafinaz@utm.my

Abstract

We report the formation of crystalline germanium dioxide (GeO_2) microclusters on *n*-Si (100) electrodeposited in non-aqueous electrolyte (a mixture of 5 vol.% germanium tetrachloride (GeCl_4) and dipropylene glycol ($\text{C}_6\text{H}_{14}\text{O}_3$)) at current density of 20 mA/cm² for 200 sec. Pt, C and Ge are used as an anode while Si acts as a cathode. Field-emission scanning electron microscopy (FESEM) images show that the deposited GeO_2 microclusters are having rounded-mushroom-shaped particles with the smallest size of 660 nm. Energy dispersive x-ray (EDX) spectra reveal that the particles are only composed of Ge and O elements. Raman spectra confirm the formation of crystalline GeO_2 with trigonal bonding structures in all samples. The photoluminescence (PL) spectra show two significant emission peaks in visible range at 2.27 eV and 2.96 eV, which seems to be attributed by GeO_2 and Si defects. $\text{C}_6\text{H}_{14}\text{O}_3$ seems to contribute to the formation of GeO_2 due to its hygroscopic nature. Such microcluster structures shall provide some potential applications for electronic and optical devices on Si platform.

Keywords: germanium dioxide, dipropylene glycol, electrochemical deposition, germanium tetrachloride, Mushroom-shaped structure

Copyright © 2017 Institute of Advanced Engineering and Science. All rights reserved.

1. Introduction

Up to date, enormous studies on crystalline Ge thin films and their nanostructures have been carried out and have been proven for excellent potential applications in electronics and optoelectronics field. Ge based compound materials, namely germanium dioxide (GeO_2) also provides significant merit to be studied in term of their properties and potential applications. GeO_2 is a blue luminescent material and exhibits high values of dielectric constant, refractive index, thermal stability and mechanical strength [1-3]. Its capability as a photosensor has been verified by optical spectroscopic methods such as Raman spectroscopy and electron spin resonance spectroscopy coupled with structural measurements [1], [4-6]. It has also been considered as one of the promising materials for optical waveguides and nanoconnections in optoelectronic communications [1, 3].

Several methods have been reported for synthesizing GeO_2 [1-3], [7-10]. Bai et al [7] reported the synthesis of GeO_2 nanowires by physical evaporation method while Wu et al [8] employed carbothermal reduction reaction. The synthesis and nanostructuring of patterned α - GeO_2 nanowires by thermal oxidation of metallic Ge was also reported by Hu et al [9]. Recently, Kim and co-workers [10] reported the catalyst free synthesis of GeO_2 nanowires by the heating of Ge powders. The synthesis of GeO_2 by the electrochemical deposition has also attained great attention. Recently, Jawad et al [3] have reported the synthesis, structural, and optical properties of electrochemically deposited GeO_2 on porous Si in a solution of germanium tetrachloride (GeCl_4) and hydrogen peroxide (H_2O_2). In their process, Pt wire was used as an anode while porous Si acted as a cathode. The current densities were varied in the range of 0.5 and 10 mA/cm². They obtained the white hexagonal, rounded or faceted monosized submicrometer crystallites with diameter of 500 nm. They showed that density of GeO_2 crystallites increase with the applied current density.

Several reports [1], [12-14] show the electrochemical deposition of Ge from the electrolyte formed by GeCl_4 and glycol. Huang et al. [14] demonstrated that Ge films and nanostructures could be deposited on n-Si using GeCl_4 in 1,3-propanediol electrolytes. Szekely [15] who pioneered the work on electrochemical deposition of Ge film from GeCl_4 in propylene glycol ($\text{C}_3\text{H}_8\text{O}_2$) electrolyte reported the metallic Ge deposition at 50 to 60 °C temperature on copper (Cu). In 2002, Saitou et al, [13] reported similar work on the deposition of Ge thin film on Cu with various durations at 300 K.

In this study, an electrochemical deposition of GeO_2 microstructures is reported. We utilized a mixture of GeCl_4 and dipropylene glycol ($\text{C}_6\text{H}_{14}\text{O}_3$) as a non-aqueous electrolyte for the electrochemical process. To the best of our knowledge no study has been conducted on the electrodeposited materials using such non-aqueous electrolyte. The results in this study show that the electrodeposited material was considerably high quality GeO_2 microstructures.

2. Research Method

An n-type phosphorus-doped Si (100) wafer with thickness: 355-405 μm and resistance: 0.7-1.3 Ωcm was used. A mixture of the as-received 5% GeCl_4 in $\text{C}_6\text{H}_{14}\text{O}_3$ (Merck, purity > 99.9%) were used as a non-aqueous electrolyte. The schematic of the electrochemical deposition setup is shown in Figure 1. The electrochemical deposition process was carried out in a simple teflon cell by using two terminal configuration where n-Si (100) substrate acts as a cathode, located at the bottom of the cell whereas three different electrodes, Pt/ C/ Ge act as an anode. The deposition was carried at room temperature in open-air ambient at a current density of 20 mA/cm^2 for 200 sec. Prior to deposition process, all samples were pre-cleaned by standard RCA process.

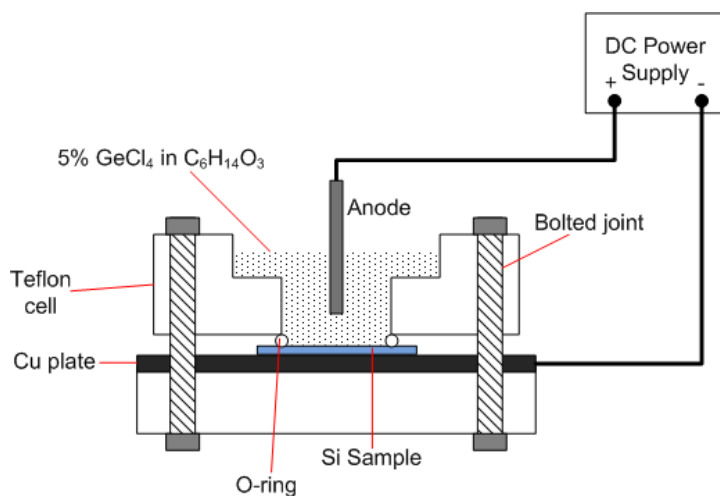


Figure 1. Schematic diagram of electrochemical deposition setup.

The deposited substance was then characterized by using field emission scanning electron microscopy (FESEM) equipped with energy dispersive x-ray (EDX) spectroscopy (FESEM JEOL JSM6701F), Raman spectroscopy (Horiba Jobin Yvon spectrometer equipped with an argon ion (Ar^+) laser of 514 nm, 20 mW) and photoluminescence (PL) spectroscopy (Horiba Jobin Yvon spectrometer equipped with HeCd laser of 325 nm).

3. Results and Analysis

3.1. FESEM and EDX Analysis

Figure 2(a), (b) and (c) shows FESEM images and EDX spectra for three samples deposited using Pt, C and Ge anode, respectively. The deposited substances show microcluster structure distributed randomly. EDX spectra reveal that the deposited substance is only composed by Ge and O element. The traces of Si observed in all samples correspond to

the Si substrate. In glance, the highest density of microclusters was obtained for sample deposited using Ge anode.

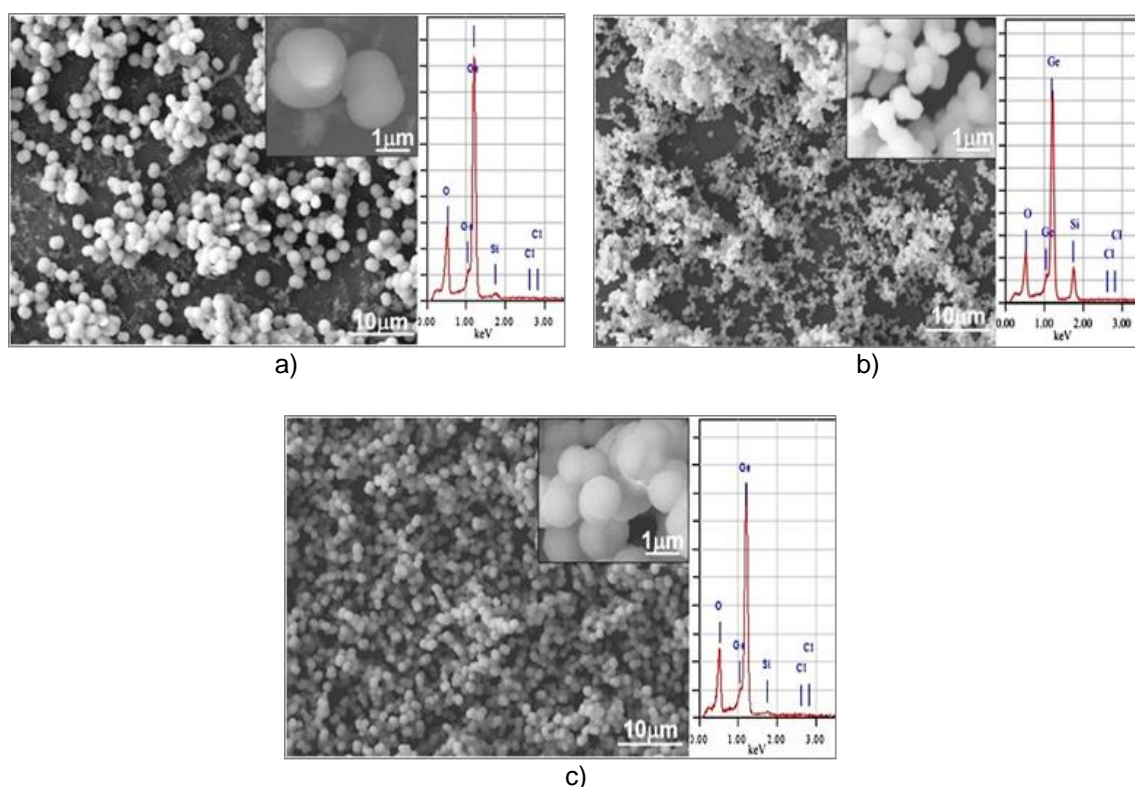


Figure 2. FESEM images and EDX spectra of deposited substance on Si with (a) Pt, (b) C and (c) Ge anode.

In term of morphological structures, it seems to show no significant difference among the samples since the grown structures shows the rounded mushroom-like shape. However, the sizes of the grown structures are different and also the density as defined by the number of clusters per unit area for the sample deposited by Ge anode is higher compared to samples with Pt and C anodes which are known to be chemically inert. At this stage, the possible reason for this is still unexplained. Since the deposition was carried out in open-air ambient, we speculated that $C_6H_{14}O_3$ has absorbed moisture from the air due to its hygroscopic nature. The hydrolysis of $GeCl_4$ with water molecules present in $C_6H_{14}O_3$ may result in the formation of GeO_2 microclusters. These GeO_2 microclusters were further confirmed by the measured Raman and PL spectra in the next section. The possible chemistry occurring in the solution due to hygroscopic effect might be denoted as follows:



We have repeated the similar experiment in air-free ambient. Here, the preparation of electrolyte and growth were carried out in nitrogen, N_2 filled glove box. It was found that no O element was detected in the grown structures [16]. Therefore, it can be said that that $C_6H_{14}O_3$ has effectively absorbed moisture from the air to generate the formation of GeO_2 .

As evident from Figure 2, the particles formed in all samples are rounded-mushroom like shaped, varying in diameter as well as the density which was defined as the number of particles per unit area. The average particle size obtained in samples deposited using Pt, C and Ge are 1.66, 0.66 and 1.49 μm , respectively. Here, the smallest particle size was observed for sample deposited using C anode. Also, at this stage, the possible reason for such result is still unexplained. Table 1 summarizes the experimental parameter and structural of the synthesized Ge with several comparisons to other similar works.

Table 1. Synthesis parameter of grown Ge structures

	Solution/Electrolyte	Electrode	Substrate	Morphological structure
This work	GeCl ₄ in dipropylene glycol	Pt/C/Ge	n-Si (100)	rounded mushroom-like with diameter 0.6-1.7μm
[3]	GeCl ₄ in H ₂ O ₂	Pt	porous Si	GeO ₂ particles with random shape, with smallest diameter 500 nm
[13]	GeCl ₄ in propylene glycol	C	Cu	mirror-like Ge film
[11]	GeCl ₄ in 1,3-propanediol	C	n-Si(100)	i) Ge film (138nm thick) ii) Ge pillars and wires with diameter 200nm and 300nm tall
[17]	HF:Ethanol based solution containing Ge species	Pt	n-Si(100)	i) flower-like Ge ii) spherical iii) uniform film layer iv) needle type

3.2. Raman and Photoluminescence (PL) Spectra Analysis

The Raman spectra obtained in the present study is shown in Figure 3 and all significant peaks are summarized in Table 2 together with previous reported data [18-19].

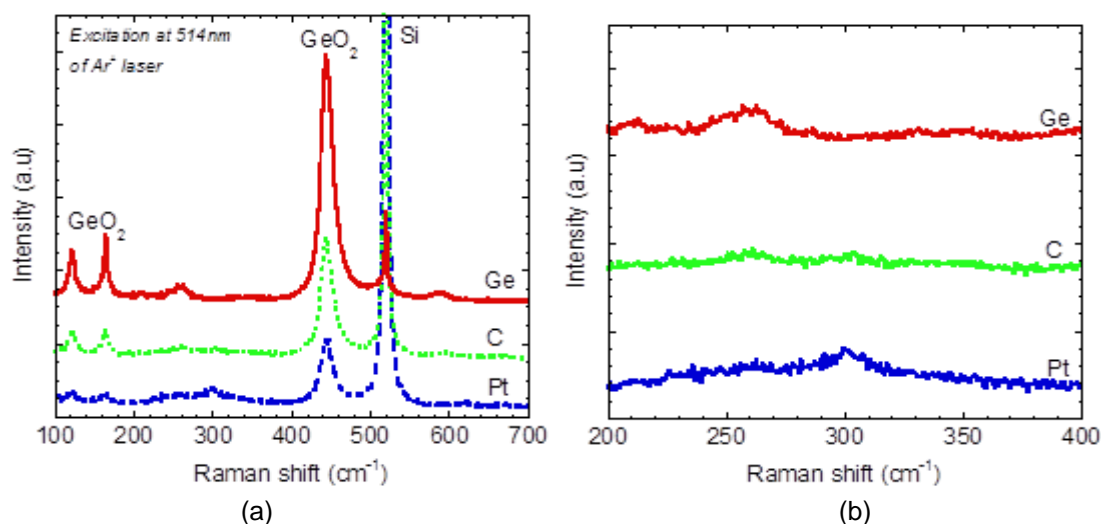


Figure 3. (a) Raman spectra of GeO₂ deposited on Si substrate using Pt, C and Ge anode and (b) enlarged Raman spectra in the range of 200-400 cm⁻¹

Table 2. Raman lines (cm⁻¹) of GeO₂ polymorphs

[18-19]	[19]	Pt	This work	
GeO ₂ (rutile)	GeO ₂ (trigonal)	GeO ₂ (trigonal)	C	Ge
			GeO ₂ (trigonal)	GeO ₂ (trigonal)
701	593	590	592	592
	583			586
	516	521	521	520
	444	443	444	445
	330			331
		300		
	263		265	263
	213	215	213	213
173				
	166	165	165	165
	123	123	123	122

A strong peak was clearly identified at 520 cm⁻¹ which corresponded to peak from Si substrate. From Figure 3(a), it can be observed that the samples deposited using Pt, C and Ge show the peaks at 443 cm⁻¹, 444 cm⁻¹, and 445 cm⁻¹, respectively, corresponding to crystalline

GeO₂. Generally, crystalline GeO₂ is observed at the peak of 444 cm⁻¹. A small shift of 1 cm⁻¹ could be due to symmetric Ge-O-Ge stretching, attributed to the optical phonon mode of nonstoichiometric Ge oxides [1].

Based on Raman lines of GeO₂ polymorphs comparison, it can be concluded that trigonal GeO₂ has been obtained for all samples in the present study. The results obtained for significant peaks are in good agreement with literature [1,19]. The small discrepancies in shifting may be attributed by the effect of complex translation and rotation of the GeO₄ tetrahedra structure [1, 19].

In further observation, the small peak at 300 cm⁻¹ was observed in the Raman spectra of Pt-anode sample as shown in Figure 3(b). Assuming that this peak is not the peak of optical phonon mode of Si at 299 cm⁻¹ but corresponds to Ge optical phonons [10, 20], we can say that the deposited GeO₂ clusters contain Ge nanocrystals. If that Ge nanocrystal is close to spherical shape, the Raman intensity can be written as [21-22]:

$$I(\omega) = A \times \sum_{i=1}^6 \int_0^1 [n(\omega_i(q)) + 1] \frac{4\pi q^2 \exp(-q^2 r_0^2 / 4)}{(\omega - \omega_i(q))^2 + (\Gamma/2)^2} dq \quad (2)$$

where $n(\omega)$ is the Bose-Einstein occupation number, $\omega_i(q)$ is the dispersion of the i th phonon branch, Γ is the line width, r_0 is the nanocrystal radius, and q is the the wave vector. The similar peak at 300 cm⁻¹ was also observed by Volodin *et al.* [22]. From the calculation using equation (2), the average radius of Ge nanocrystal was estimated to be around 1.3 nm [22]. The presence of Ge nanocrystalline in GeO₂ may leads to an interesting application as this kind of structure can be possibly used in optoelectronic devices [22].

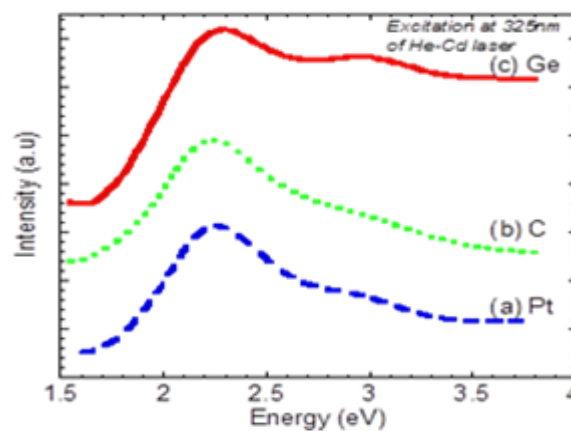


Figure 4. Photoluminescence Spectra of GeO₂ Deposition on Si Substrate Using Pt, C and Ge Anode.

Figure 4 shows PL emission spectra of samples deposited using Pt, C and Ge anode, respectively. The two peaks including one significant at 2.27 eV (546.8 nm in green region) and a shoulder at 2.96 eV (418.8 nm in blue region) can be observed. The two peaks in PL spectra obtained in this study, are slightly similar as reported by Kim *et al.* [10]. In their work [10], the PL spectra was best fitted with two Gaussian functions centered at 2.45 eV and 2.91 eV. They suggested that blue and green light emissions originated from radiative recombination with regard to defects in GeO₂, including oxygen vacancies and oxygen-germanium vacancy centers.

The visible band around 2.27 eV indicated the different types of defects in Si [23]. In addition, Gao *et al.* [24] has ruled out on emission probability of quantum confinement in visible region on Ge nanocrystals which indicate that 2.9 eV can also be attributed to the transition from triplet to singlet in GeO₂ defects containing two non-bonding electrons [23],[25]. The

transition from singlet to singlet forms the ground state of defect. This excitation is related to the presence of Ge and O as a clear trend of stronger blue PL is usually observed with the increase of O/Ge ratio. Thus, GeO₂ with weak blue PL peak might indicate that it contains more Ge-O related defect.

4. Conclusion

Electrochemical deposition using the mixture GeCl₄ and C₆H₁₄O₃ in open air ambient seems to contribute to the formation of GeO₂ microclusters. Due to hygroscopic nature of C₆H₁₄O₃, the water molecule from the air will be absorbed and then react with the GeCl₄ with the passage of electricity to form GeO₂ clusters to be deposited on the substrate. The all deposited rounded-mushroom-shaped GeO₂ microclusters show trigonal bonding structure with the smallest size of 660 nm. The deposited GeO₂ microcluster with embedded Ge nanocrystalline structures shall provide some potential applications for electronic and optical devices on Si platform.

References

- [1] Atuchin VV, Gavrilova TA, Gromilov SA, Kostrovsky VG, Pokrovsky LD, Troitskaia IB, Vemuri RS, Carbajal-Franco G, Ramana CV. Low-temperature chemical synthesis and microstructure analysis of GeO₂ crystals with α -quartz structure. *Crystal Growth and Design*. 2009; 9 (4): 1829–1832.
- [2] Yan WX, Lian D, Fang DG, Peng W, Wei W, Duo WL, Yong Q. Synthesis and characterization of nano/microstructured crystalline germanium dioxide with novel morphology. *Chinese Science Bulletin*. 2009; 2810–2813.
- [3] Jawad MJ, Hashim MR, Ali NK. Synthesis, structural, and optical properties of electrochemically deposited GeO₂ on porous silicon. *Electrochemical and Solid-State Letters*. 2011; 14 (2): D17–D19.
- [4] Terakado N, Tanaka K. Photo-induced phenomena in sputtered GeO₂ films. *Journal of Non-Crystalline Solids*. 2005; 351: 54–60.
- [5] Zhou M, Shao L, Miao L. Matrix Isolation Infrared Spectroscopic and Density Functional Theoretical Calculations of the GeO₂⁻ and GeO₄⁻ Anions. *Journal of Physical Chemistry A*. 2002; 106: 6483-6486.
- [6] Terakado N, Tanaka K. Photo-induced phenomena in GeO₂ glass. *Journal of Non-Crystalline Solids*. 2006; 352 (36–37): 3815-3822.
- [7] Bai ZG, Yu DP, Zhang HZ, Ding Y, Wang YP, Gai XZ, Hang QL, Xiong GC, Feng SQ. Nano-scale GeO₂ wires synthesized by physical evaporation. *Chemical Physics Letters*. 1999; 303: 311–314.
- [8] Wu XC, Song WH, Zhao B, Sun YP, Du JJ. Preparation and photoluminescence properties of crystalline GeO₂ nanowires. *Chemical Physics Letters*. 2001; 349: 210–214.
- [9] Hu JQ, Li Q, Meng XM, Lee CS, Lee, ST. Synthesis and nanostructuring of patterned wires of α -GeO₂ by thermal oxidation. *Advanced Materials*. 2002; 14 (19): 1396–1399.
- [10] Kim HW, Lee JW, Kebede MA, Kim HS, Lee C. Catalyst-free synthesis of GeO₂ nanowires using the thermal heating of Ge powders. *Current Applied Physics*. 2009; 9: 1300–1303.
- [11] Huang Q, Bedell S., Saenger KL, Copel M, Deligianni H, Romankiwa LT. Single-crystalline germanium thin films by electrodeposition and solid-phase epitaxy. *Electrochemical and Solid-State Letters*. 2007; 10 (11): D124-D126.
- [12] Szekely, G. Electrodeposition of Germanium. *Journal of the Electrochemical Society*. 1951; 98 (8): 318–324.
- [13] Saitou M, Sakae K, Oshikawa. Evaluation of crystalline germanium thin films electrodeposited on copper substrates from propylene glycol electrolyte. *Surface and Coatings Technology*. 2002; 162: 101–105.
- [14] Huang Q, Deligianni H, Romankiwa LT. Anisotropic growth of nanostructures in germanium electroplating. *Electrochemical and Solid-State Letters*. 2007; 10 (11): D121-D123.
- [15] Szekely, G. *Electroplating of Germanium*. Patent US2690422. 1951.
- [16] Abidin MSZ, Shahjahan, Mahmood MR, Nayan N, Hashim AM. *Synthesis of high purity Ge on Si substrate by electrochemical deposition for the growth of Ge-on-insulator (GOI) structures*. ThinFilms 2012. 14-17 July 2012.
- [17] Jawad MJ, Hashim MR, Ali NK, C´orcoles EP, Sharifabad ME. An alternative method to grow Ge thin films on Si by electrochemical deposition for photonic applications. *Journal of the Electrochemical Society*, 2012; 159 (2): D124-D128, 2012.
- [18] Scott JF. Raman Spectra of GeO₂. *Physical Review B*. 1970; 1 (8): 3488–3493.
- [19] Micoulaut M, Cormier L, Henderson GS. The structure of amorphous, crystalline and liquid GeO₂. *Journal of Physics: Condensed Matter*. 2006; 18: R753–R784.

- [20] Kartopu G, Bayliss SC, Karavanskii VA, Curry RJ, Turan R, Sapelkin AV. On the origin of the 2.2–2.3eV photoluminescence from chemically etched germanium. *Journal of Luminescence*. 2003; 101 (4): 275-283.
- [21] Paillard V, Puech P, Laguna MA, Carles R, Kohn B, Huisken F. Improved one-phonon confinement model for an accurate size determination of silicon nanocrystals. *Journal of Applied Physics*. 1999; 86 (4): 1921-1924.
- [22] Volodin V, Gorokhov E, Efremov M, Marin D, Orekhov D. Photoluminescence of GeO₂ films containing germanium nanocrystals. *JETP Letters*. 2003; 77 (8): 411-414.
- [23] Zacharias M, Fauchet PM. Light emission from Ge and GeO nanocrystals. *Journal of Non-Crystalline Solids*. 1998; 227: 1058–1062.
- [24] Gao T, Tong S, Zheng X, Wu X, Wang L, Bao X. Strong visible photoluminescence from Ge/porous Si structure. *Applied Physics Letters*. 1998; 72 (25): 3312-3313.
- [25] Ko TS, Shieh J, Yang MC, Lu TC, Kuo HC, Wang SC. Phase transformation and optical characteristics of porous germanium thin film. *Thin Solid Films*. 2008; 516 (10): 2934-2938.